Mon. Not. R. Astron. Soc. **389,** 799–805 (2008) doi:10.1111/j.1365-2966.2008.13580.x

Infrared and millimetre-wavelength evidence for cold accretion within a $z = 2.83$ Lyman α blob

Daniel J. B. Smith,[1,2⋆] Matt J. Jarvis,[3] Mark Lacy[4] and Alejo Martínez-Sansigre[5]

[1]*Astrophysics Research Institute, Liverpool John Moores University, Twelve Quays House, Egerton Wharf, Birkenhead CH41 1LD*
[2]*Department of Astrophysics, University of Oxford, Denys Wilkinson Building, Keble Road, Oxford OX1 3RH*
[3]*Centre for Astrophysics, Science & Technology Research Institute, University of Hertfordshire, Hatfield, Herts AL10 9AB*
[4]*Spitzer Science Center, California Institute of Technology, Pasadena, CA 91125, USA*
[5]*Max-Planck-Institut für Astronomie, Königstuhl 17, D-69117 Heidelberg, Germany*

Accepted 2008 June 13. Received 2008 June 12; in original form 2008 April 25

ABSTRACT

This paper discusses infrared and millimetre-wavelength observations of a Lyman α blob (LAB) discovered by Smith & Jarvis, a candidate for ionization by the cold accretion scenario discussed in Fardal et al. and Dijkstra et al. We have observed the counterpart galaxy at infrared wavelengths in deep observations with the *Spitzer Space Telescope* using the IRAC 3.6, 4.5, 5.8 and 8.0 μm and MIPS 24 μm bands, as well as using the Max-Planck Millimeter Bolometer (MAMBO-2) at a wavelength of 1.2 mm with the IRAM 30 m telescope. These observations probe the $\gtrsim$95 kpc Lyman α halo for the presence of obscured active galactic nucleus (AGN) components or the presence of a violent period of star formation invoked by other models of ionization for these mysterious objects. 24 μm observations suggest that an obscured AGN would be insufficiently luminous to ionize the halo, and that the star formation rate within the halo may be as low as $<140\,\mathrm{M_\odot\,yr^{-1}}$ depending on the model spectral energy distribution (SED) used. This is reinforced by our observations at 1.2 mm using MAMBO-2, which yield an upper limit of star formation rate $<550\,\mathrm{M_\odot\,yr^{-1}}$ from our non-detection to a 3σ flux limit of 0.86 mJy beam^{-1}. Finding no evidence for either AGN or extensive star formation, we conclude that this halo is ionized by a cold accretion process. We derive model SEDs for the host galaxy, and use the Bruzual & Charlot and Maraston libraries to show that the galaxy is well described by composite stellar populations of total mass $3.42 \pm 0.13 \times 10^{11}$ or $4.35 \pm 0.16 \times 10^{11}\,\mathrm{M_\odot}$ depending on the model SEDs used.

Key words: galaxies: haloes – galaxies: high-redshift.

1 INTRODUCTION

Lyman α blobs, discovered by Steidel et al. (2000), consist of amoebic structures emitting profusely at the rest-frame wavelength of the Lyman α emission line, 1216 Å. Whilst these very large Lyman α emitting haloes are reminiscent of the extended emission line regions observed around powerful high-redshift radio galaxies (e.g. Villar-Martín 2007), they typically have less than 1 per cent of the associated radio flux, raising the question as to what ionizes the neutral hydrogen in order to enable the emission of Lyman α photons. Three of the most plausible explanations for this are as follows.

(i) Lyman α blobs (LABs) contain hidden QSOs (e.g. Haiman & Rees 2001; Weidinger, Møller & Fynbo 2004; Weidinger et al. 2005; Barrio et al. 2008). The luminous nature of LABs with typically $L = 10^{44}\ \mathrm{erg\,s^{-1}}$ in the Lyman α emission line alone suggests that the hard spectra and bolometric luminosity of QSOs are prime candidates to power such a galaxy's emission.

(ii) The Lyman α emission comes from a dust-enshrouded, extreme starburst galaxy with a large-scale superwind due to large numbers of luminous and short-lived OB stars (e.g. Taniguchi & Shioya 2000; Ohyama et al. 2003; Wilman et al. 2005; Matsuda et al. 2007). Observational evidence from, for example, Chapman et al. (2001) and Geach et al. (2007) associating LABs with submillimetre galaxies suggests that some LABs contain enshrouded starbursts forming stars at rates of $\sim 1000\,\mathrm{M_\odot\,yr^{-1}}$.

(iii) We are observing the cooling radiation of a collapsing protogalaxy inside a dark matter halo's gravitational potential (the so-called 'cold accretion' model – for example, Haiman, Spaans & Quataert 2000; Fardal et al. 2001; Matsuda et al. 2004; Dijkstra, Haiman & Spaans 2006a,b; Nilsson et al. 2006; Dijkstra 2007; Smith & Jarvis 2007). A cold accretion scenario invokes collisional

⋆E-mail: djs@astro.livjm.ac.uk

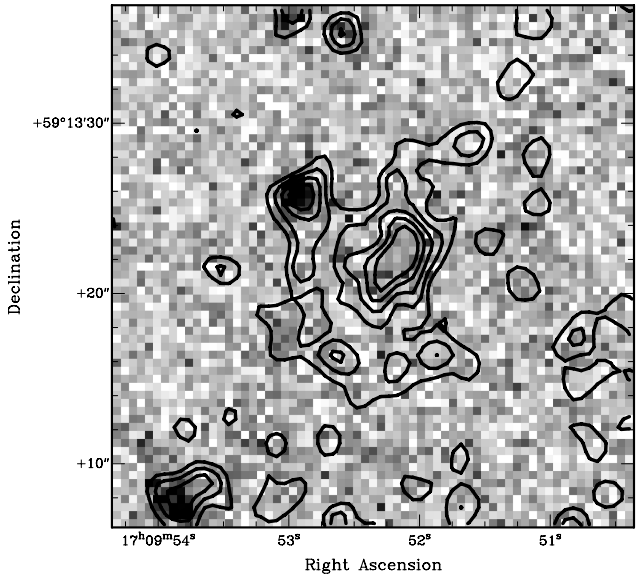

Figure 1. Narrow-band contour map overlaid on the Sloan-g' band data. This frame is ∼33 arcsec on a side and north is up while east is to the left-hand side. The object to the north and east of the core of the Lyman α emission is a low-redshift interloper, identified as being at $z = 0.84$ due to the presence of [O II]$_{3727}$, [Ne IV]$_{2424}$, Mg II$_{2799}$ and [C II]$_{2326}$ emission in our optical spectroscopy (for more details see Smith & Jarvis 2007).

excitation and re-radiation of accreting neutral gas to power the profuse Lyman α emission extended over the halo.

The sources of ionization residing within these galaxies (which are sometimes extended over many tens of kiloparsecs) are currently thought to be diverse. This result is due to the discovery of a 200 kpc LAB in Dey et al. (2005) associated with a 24 μm detection attributed to an obscured AGN, to the discovery by Chapman et al. (2001) of a highly luminous submillimetre source (with $L_{\rm bol} \sim 10^{13}\,{\rm L}_{\odot}$) indicative of a very high star formation rate ($\sim 1000\,{\rm M}_{\odot}\,{\rm yr}^{-1}$) residing within LAB1 from Steidel et al. (2000), and to the non-detection of any apparent source of ionization associated with a LAB in the GOODS-South field by Nilsson et al. (2006).

Smith & Jarvis (2007) discovered only the second known Lyman α blob thought to be ionized by the process of cold accretion, residing at $z = 2.83$. In Fig. 1, we show the Sloan-g' band image of the LAB from our survey, overlaid with a contour map of the He II narrow-band data, sensitive to Lyman α emission at the redshift of the LAB. This LAB was found to be extended over at least $\gtrsim$95 kpc, with a Lyman α luminosity of $L_{{\rm Ly}\alpha} = 2.1 \pm 0.5 \times 10^{43}\,{\rm erg\,s}^{-1}$.

The LAB in question is located at $17^{\rm h}09^{\rm m}52\overset{\rm s}{.}3$ $+59^{\circ}13'21\overset{''}{.}72$ (J2000), on the very edge of the extragalactic component of the *Spitzer* First Look Survey (Marleau et al. 2004; Fadda et al. 2006), and was covered with any signal-to-noise ratio (S/N) at all only in the 4.5 μm band (IRAC channel 2 – Lacy et al. 2005). In any case, the FLS observations were not deep enough for the type of study proposed here (see below).

AGN themselves are expected to be particularly dusty due to the torus invoked by schemes of AGN unification (Antonucci 1993) to explain the different observed species; this also makes them bright at mid-infrared (mid-IR) wavelengths since the warm torus is thought to reprocess the X-ray and ultraviolet (UV) photons emitted by the central engine. Indeed, through their mid-IR emission, powerful AGN (quasars) can be identified up to high redshifts (e.g. Lacy et al. 2004; Martínez-Sansigre et al. 2005), even when they are so heavily obscured that they are undetected at X-ray energies (e.g. Polletta et al. 2006; Lacy et al. 2007; Martínez-Sansigre et al. 2007).

In the event that there is a 24 μm detection residing within the LAB, through studying its IR spectral energy distribution (SED) we would be able to distinguish between an obscured AGN and the starburst SED that would be expected if there was extensive ongoing star formation in the LAB counterpart galaxy.

LABs ionized by a starburst are found to have very high star formation rates based on their fluxes at submillimetre wavelengths equivalent to $\sim 1000\,{\rm M}_{\odot}\,{\rm yr}^{-1}$ (e.g. Chapman et al. 2001; Geach et al. 2007). The recent high-resolution Submillimetre Array (SMA) observations of Matsuda et al. (2007) did not detect LAB1 from Steidel (2000), despite the bright submillimetre continuum measured by Chapman et al. (2001). Matsuda et al. (2007) argued that the submillimetre continuum was most likely resolved out by the high spatial resolution interferometric SMA observations, suggesting that the spatial extent of the submillimetre emitting region was $\gtrsim$30 kpc, comparable to the extent of the Lyman α emission itself. This reinforces the superwind model for this LAB, in which rapid star formation within the halo is widely distributed, and could be powering the Lyman α emission. Observing this new halo from Smith & Jarvis (2007) at millimetre wavelengths then provides an additional constraint on the properties of the ionizing source residing within.

Here, we present the results of two independent tests for the presence of starbursting or AGN components enshrouded within the structure. This paper is organized as follows. In Section 2, we describe our *Spitzer Space Telescope* and MAMBO-2 observations, while in Section 3 we present our results, including our improved constraints on this galaxy's SED, and Section 4 presents our conclusions. Throughout this paper, the *AB* magnitude system is used (Oke & Gunn 1983), and a standard cosmology is assumed in which $H_0 = 71\,{\rm km\,s}^{-1}$, $\Omega_{\rm M} = 0.27$ and $\Omega_{\Lambda} = 0.73$ (Dunkley et al. 2008).

2 OBSERVATIONS

2.1 *Spitzer Space Telescope* observations

We observed the region centred on this LAB in 21 dithered 30 s exposures in Infrared Array Camera (IRAC) channels 1 and 3 and 33 times 30 s in IRAC channels 2 and 4 ($10^{1}/_{2}$ and $16^{1}/_{2}$ min in total, respectively). We designed our 24 μm Multiband Imaging Photometer for *Spitzer* (MIPS) observations to use a seven-point jittering positional offset algorithm with offsets corresponding to the six nodes of a hexagon, plus the central position. We observed at each position for 501 s, resulting in a total of 3507 s on source. The jittering pattern was employed to ensure effective chip artefact rejection, and result in a reasonably uniform depth over the central 5 arcmin of the field of view. No new MIPS channel 2 and 3 data were acquired.

These observations were carried out under programme number 40957; the IRAC data in channels 1 and 3 were observed on 2007 August 8, with channels 2 and 4 observed on August 12 and the MIPS 24 μm data observed on August 22. The raw data were reduced, and photometric and astrometric solutions were applied automatically using the Spitzer Science Centre pipeline version S16.1.0. The resulting frames are calibrated to units of surface brightness (MJy sr^{-1}). The reduced IRAC images, centred on the LAB counterpart galaxy (circled in black) can be seen in Fig. 2.

The MIPS pipeline-reduced frames were reduced in seven separate parent images due to the target jitter pattern employed. They

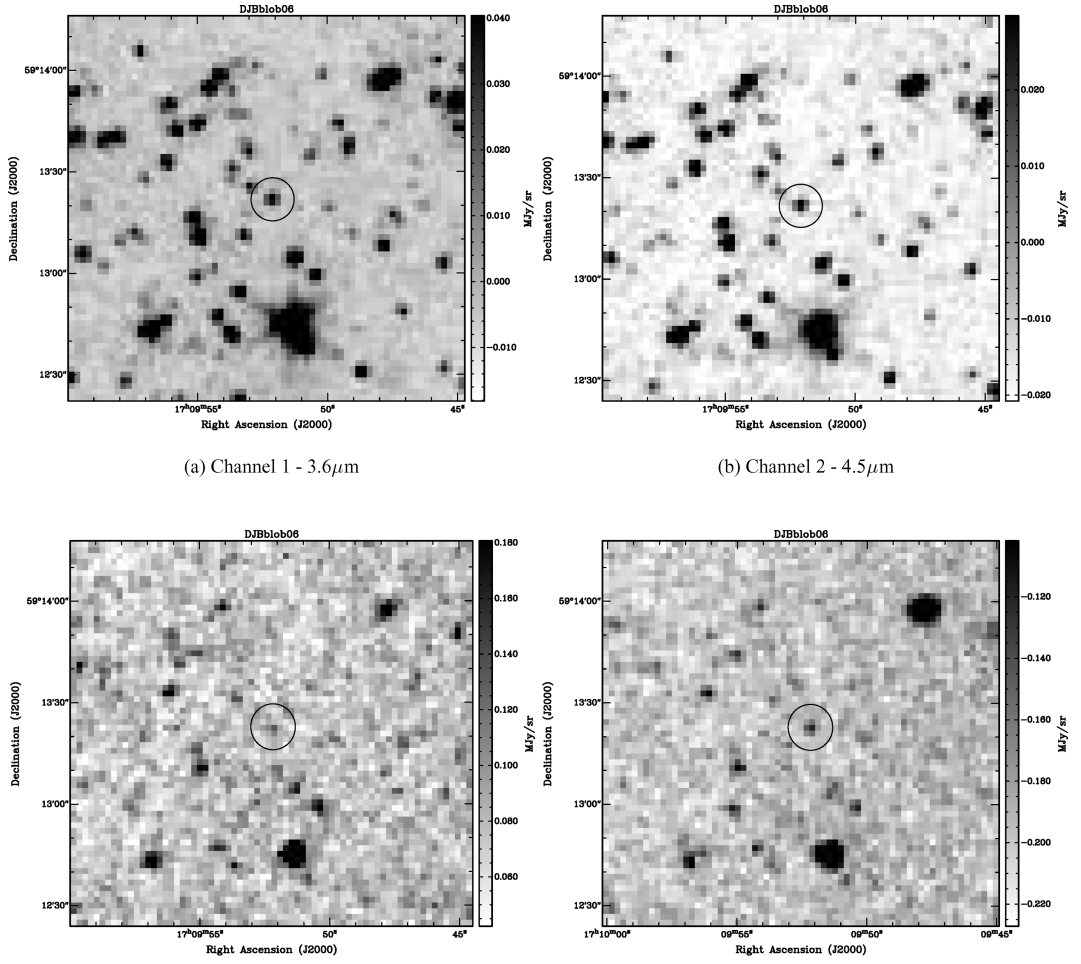

(a) Channel 1 - 3.6μm

(b) Channel 2 - 4.5μm

(c) Channel 3 - 5.8μm

(d) Channel 4 - 8.0μm

Figure 2. IRAC observations of the LAB counterpart galaxy. The galaxy is centred in each frame and identified by the 12 arcsec diameter black circle. The counterpart galaxy is clearly detected in each band; for fluxes and errors, see Table 1.

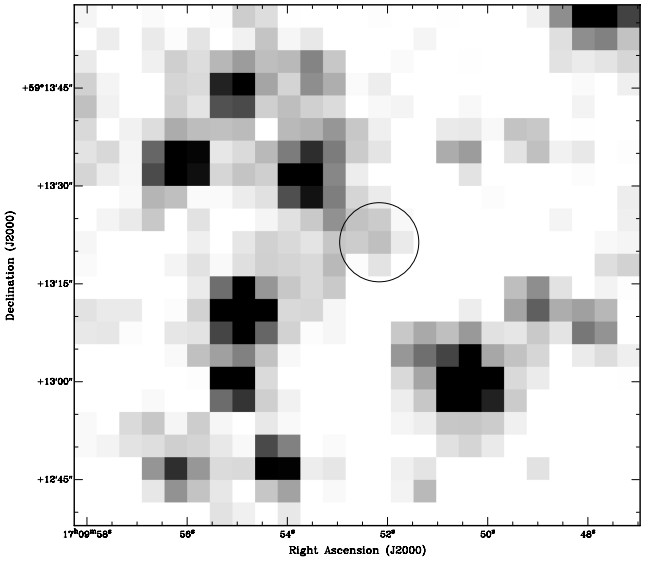

Figure 3. MIPS channel 1 (24 μm) observations centred on the LAB counterpart galaxy (circled). The galaxy is only marginally detected in this band (i.e. at $<3\sigma$); see Section 3. The circle is 12 arcsec in diameter.

were aligned according to their astrometric solutions using the IRAF task WREGISTER, before being stacked using IMCOMBINE (also in IRAF). The stacked MIPS data centred on the position of the LAB (again circled in black) are displayed in Fig. 3.

To extract meaningful fluxes from the IRAC/MIPS data, a conversion factor must be applied to convert from MJy sr^{-1} to something more useful, usually μJy pixel^{-1}. The conversion factor must take into account both the difference between MJy and μJy, and the difference between a steradian and the area of each pixel (see http://ssc.spitzer.caltech.edu/fls/ for further details). Since *Spitzer* IRAC imaging data are calibrated to known standard source observations measured in 10 arcsec apertures (for MIPS, this is 35 arcsec), some correction to the photometry is necessary when measuring fluxes though apertures of different sizes due to the varying amounts of the point spread function (PSF) falling within the extent of the aperture. For a 4 arcsec radius aperture in IRAC, this factor has values of 1.074, 1.075, 1.080 and 1.150 for channels 1 to 4 (3.6–8.0 μm), whereas for MIPS channel 1 (24 μm band), the factor is ∼2.4, due to the much larger PSF in MIPS data.

The MIPs 24 μm data have a 5σ detection limit varying from ∼27.4 μJy at the centre of the field of view to ∼58 μJy towards the edges. We have the sensitivity to detect star formation rates (SFRs) as low as 200 $M_\odot$ yr^{-1} at 5σ in our 24 μm data (although this does depend on the exact SED assumed, due to the relationship

between 24 μm flux and far-IR luminosity), and the accompanying IRAC sensitivity to distinguish between AGN and starbursting components, were they detected in the 24 μm band.

2.2 MAMBO-2 observations

The Lyman α halo was observed between 2008 January 19 and March 3 using the Max-Planck Millimetre Bolometer (MAMBO-2, Kreysa et al. 1998) instrument at the Institut de Radio Astronomie Millimétrique (IRAM) 30 m telescope at Pico de Veleta, Spain. The effective frequency of MAMBO-2 is 250 GHz, which corresponds to 1.2 mm, with a beam full width at half-maximum (FWHM) of 10.7 arcsec. The observations were carried out in mostly clear conditions with atmospheric opacity $\tau_{1.2\,\mathrm{mm}} < 0.3$ and low sky noise ($<$70 mJy beam^{-1}, with most of the scans having $\leq$40 mJy beam^{-1}). The targets were centred on the most sensitive pixel (number 20) and standard on-off observations were carried out with a wobbler throw in azimuth of 35–45 arcsec, at a rate of 2 Hz to enable effective sky subtraction. Individual scans of typically 20 min were carried out, and the total integration time was 212 min.

To enable effective sky subtraction, reduce systematic errors and avoid false positive detections, we varied the wobbler throw between 35, 40 and 45 arcsec, and scans were conducted at different times on different days. As a result, it is very unlikely for the sky observations to repeatedly fall on bright nearby sources. Prior to each scan, pointing corrections were made by observing a nearby bright source, J1638+573. The focus and opacity were checked regularly (typically every 2 h) and the focus was generally found to be stable. Gain calibration was performed using Neptune, Uranus or Mars, and monitored regularly using very bright millimetre sources (typically $\geq$5 Jy); the resulting absolute flux scale has an uncertainty of ±20 per cent. The data were reduced by using the MOPSIC software (Zylka 1998); with these new data we have the sensitivity to effectively distinguish between the three most plausible sources of ionization.

3 RESULTS

Due to the crowded nature of the field around the LAB caused by the depth of the data, 4 arcsec apertures were preferred over larger options to prevent the inclusion of flux from neighbouring sources (although this was not possible for the MAMBO-2 observations, due to the 10.7 arcsec FWHM of the beam). The fluxes were calculated using the function APER from the IDL Astronomy Users' Library,[1] which computes photometry in specified apertures and background annuli. APER accounts precisely for the different contributions of different square pixels overlapping on circular apertures, of greater importance here due to the comparatively large pixel size (1.2 arcsec). Photometry of the LAB counterpart is presented in Table 1.

Table 1. Photometric data for the LAB. Magnitudes are measured in apertures with 4 arcsec radii (with the exception of the 1.2 mm data, for which the beam FWHM is 10.7 arcsec), and where they are limits, they are to 1σ. The 1.2 mm flux is calculated as detailed in the text, while the radio limits are calculated according to the local rms noise in the images. The large error in the He II narrow-band filter has several causes; the faintness of the LAB, the difficulty in fitting the sky background due to the very extended nature of the LAB and the presence of the nearby low-z interloper to the north and east of the LAB counterpart galaxy all contribute. Some values for the longer wavelength data are given in units of Jansky (1 Jy = 10^{-26} W Hz^{-1}), which is deemed more appropriate.

Photometric band	*AB* Magnitude/Flux
u*	$>$26.44
U	$>$27.85
Harris *B*	$23.57^{+0.23}_{-0.19}$
Sloan-g'	$23.97^{+0.70}_{-0.43}$
He II (468.6)	$22.16^{+1.46}_{-0.60}$
Harris *V*	$23.97^{+0.32}_{-0.25}$
R	$23.81^{+0.20}_{-0.17}$
Sloan-i'	$24.07^{+1.19}_{-0.55}$
J	> 19.74
K	$21.05^{+0.20}_{-0.18}$
3.6 μm	$20.71^{+0.04}_{-0.04}$
4.5 μm	$20.63^{+0.05}_{-0.04}$
5.8 μm	$20.85^{+0.36}_{-0.27}$
8.0 μm	$20.62^{+0.24}_{-0.19}$
24 μm	18.69 ± 7.37 μJy
1.2 mm	$<$290 μJy
1.4 GHz	$<$20 μJy
610 MHz	$<$80 μJy

3.1 Searching for an obscured AGN within the LAB

To consider the possibility of an AGN residing within the halo, we examine the results of our 24 μm channel MIPS observations. Table 1 and Fig. 3 demonstrate the marginal detection at the position of the LAB in the MIPS 24 μm band of 18.69 ± 7.37 μJy (or in *AB* magnitudes, $m_{24\,\mu\mathrm{m}} = 20.72^{+0.54}_{-0.36}$). The object is barely detected, and confusion noise is the dominant source of noise in the flux estimate. The error in this band was estimated using blank field aperture measurements of nearby regions of sky with a similar background of confusing sources. This technique was used to derive the 24 μm photometry in preference to PSF fitting since the errors are more easily estimated (in particular, estimating the true background is almost impossible in these data due to the effects of confusion). If this marginal detection is real, it may be indicative of an obscured AGN component or an ongoing starburst residing within the halo.

To quantify the likelihood that this detection in the 24 μm band observations is real, we turn to Gaussian statistics. This value can be obtained by chance approximately 1.1 per cent of the time given the error associated with the measurement, however this value must be treated as a lower limit due to the presence of nearby sources whose PSFs overlap with the 4 arcsec flux extraction aperture used for this measurement.

We adopt the conservative assumption that the 24 μm detection is real in order to estimate the possibility of an AGN or a starburst being the power source of the extended Lyman α emission. In this way, we can estimate a limiting luminosity for any AGN residing in the LAB from the 24 μm flux density, which is not thought to be affected by dust obscuration. If this marginal detection were entirely due to an AGN, the monochromatic luminosity would correspond to a rest-frame luminosity of $L_{\nu_{\mathrm{RF}}} = 3 \times 10^{23}$ W Hz^{-1} at

[1] http://idlastro.gsfc.nasa.gov/

$\lambda_{RF} = 6.3\,\mu$m. Assuming the Elvis et al. (1994) quasar SED, we estimate that this corresponds to $L_{bol} = 3.4 \times 10^{11}\,L_{\odot}$ (1.3×10^{45} erg s^{-1}), of which $\sim 8.6 \times 10^{43}$ erg s^{-1} is emitted at wavelengths between 200 and 912 Å in the rest frame, and thus capable of powering Lyman α emission (following Dey et al. 2005, and assuming case B recombination).

At a first glance, it seems plausible that an unobscured AGN is energetically capable of powering a reasonable proportion ($\sim$30 per cent) of the $2.83 \pm 0.5 \times 10^{44}$ erg s^{-1} Lyman α emission that we observe. However, we can also use a photon number counts argument similar to that in Neugebauer et al. (1980) to test the possibility of the halo being ionized by an AGN. The Lyman α luminosity of the halo requires a total of 1.7×10^{55} ionizing photons per second. Integrating under the Elvis et al. (1994) quasar, SED between 200 and 912 Å (it is only these photons which contribute to the ionization of neutral hydrogen, and thus plausibly power the Lyman α emission) suggests that any putative quasar component may emit only 2.3×10^{54} photons each second. This figure is almost an order of magnitude fewer than that required to result in the Lyman α luminosity that we observe. It seems improbable that an AGN is powering the LAB; the quasar SED normalized to our 24 μm detection is displayed in Fig. 4.

Furthermore, it should be noted that LABs containing AGN (e.g. which was presented in Dey et al. 2005) and similarly luminous Lyman α haloes belonging to some high-redshift radio galaxies at $z > 2$ (e.g. Villar-Martín 2007, compared with 24 μm data from Seymour et al. 2007) are detected at mid-IR wavelengths at fluxes typically at least an order of magnitude more luminous than those probed by our 24 μm observations. Our view that an AGN is not responsible for the Lyman α emission observed here is further supported by the lack of other evidence for an AGN at radio wavelengths in the Giant Metrewave Radio Telescope (GMRT) and Very Large Array (VLA) data (at 610 MHz and 1.4 GHz, respectively), or in our optical spectroscopy, where no other emission lines were detected (see Smith & Jarvis 2007).

3.2 Constraining the star formation rate with MAMBO-2 and MIPS

To probe for evidence of the obscured SFRs implied by superwind models of LABs of the order of $\sim 1000\,M_{\odot}$ yr^{-1} (e.g. Taniguchi & Shioya 2000), we turn first to the results of our MAMBO-2 observations. The host galaxy is not detected at 1.2 mm down to a 3σ flux limit of 0.86 mJy. To constrain the SFR probed due to cold dust masses within this halo, we consider the 1.2 mm (observed frame) flux to be due to a *grey body*, with emissivity of the form given in equation (1) which is also displayed in Fig. 4:

$$F_{\lambda} \propto \frac{1}{\lambda} \frac{\frac{1}{\lambda}^{(4+\beta)}}{e^{(\frac{hc}{\lambda kT})} - 1}, \quad (1)$$

where β corresponds to the emissivity index of the grey body spectrum and T to the temperature of the dust. We assume typical values for these two parameters from Omont et al. (2003) of $\beta = 1.5$ and $T = 45$ K, and adopt a conversion from far-IR luminosity between 8 and 1000 μm, and SFR following Kennicutt (1998). With these assumptions, we find that our 3σ flux limit at 1.2 mm suggests that the SFR within the LAB is $<550\,M_{\odot}$ yr^{-1}. This puts our 3σ upper limit for the SFR within this LAB slightly below the SFRs required by superwind models of LAB ionization. If we adopt a slightly lower temperature for the dust component, $T = 35$ K, our estimate for the SFR within the halo becomes $<220\,M_{\odot}$ yr^{-1} to 3σ.

We can also use our MIPS observations to constrain the SFR. To obtain SFR estimates from 24 μm fluxes, one must assume a particular SED in order to enable an estimate of the far-IR

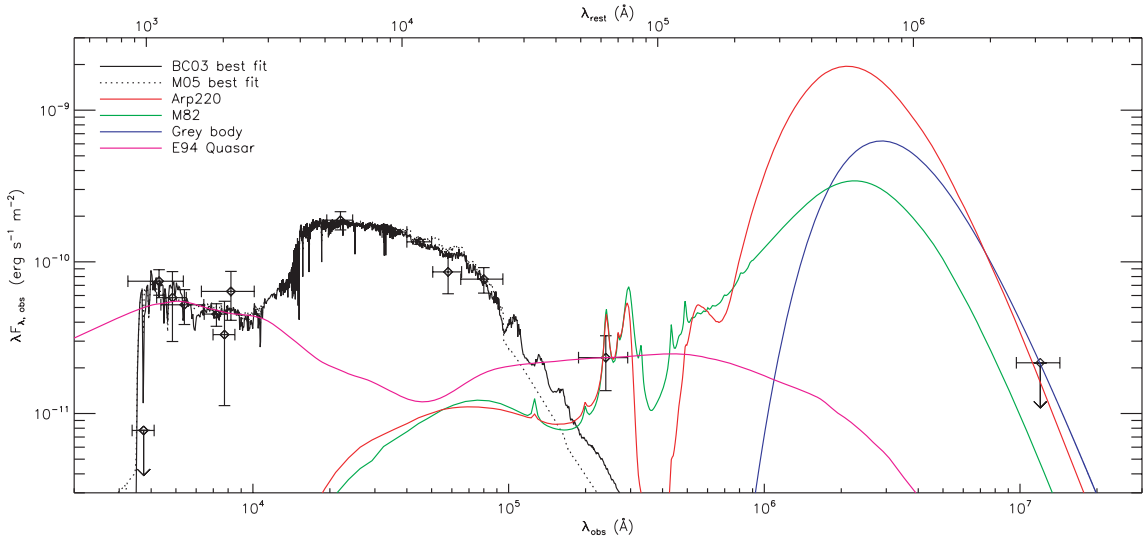

Figure 4. Multiwavelength spectral energy distribution of the LAB's counterpart galaxy. The best-fitting models to our photometry from the Bruzual–Charlot and Maraston simple stellar population models (solid and dotted black lines, respectively). Also included are Arp 220, M82 and template QSO (from Elvis et al. 1994) SEDs shown in red, green and purple, respectively, and the best-fitting grey-body emission profile (blue). The Bruzual & Charlot (2003) and Maraston (2005) SEDs are normalized to the 3.6 μm band, the Arp 220, M82 and QSO templates are normalized to the 24 μm band and the grey body is normalized to the 1.2 mm MAMBO-2 observations. We find that our optical and IRAC data are very well described by a composite simple stellar population consisting of a young and an old component aged 10 Myr and 0.8 Gyr for the Bruzual & Charlot (2003) models, or 10 Myr and 2.0 Gyr for the Maraston (2005) models. The weak detection at 24 μm, which is questionable due to its low S/N as well as the approaching confusion limit, indicates either a weak obscured AGN component or a starburst. Our other data strongly constrain these possibilities – see the text. While the unobscured template quasar SED is consistent with our optical photometry, it is inconsistent with the results of our spectroscopy, which do not detect the presence of the high-ionization emission lines that the presence of such a naked AGN would suggest.

luminosity and then proceed as for the *grey-body* models. Instead of assuming a *grey-body* SED, here we use templates for M82 and Arp 220 from Siebenmorgen & Krügel (2007) to derive SFR estimates. If our detection at 24 μm is real, then it corresponds to SFRs of ∼140 (M82 template) or 620 (Arp 220 template) $M_\odot\,yr^{-1}$. Given the uncertainties in these estimates, both values are consistent with the limit derived from our MAMBO-2 observations.

3.3 The stellar population

Having essentially ruled out the presence of a powerful AGN, we turn our attention to the stellar population of the LAB. The new IRAC photometry of the LAB counterpart galaxy provides much better constraints for its stellar SED, enabling us to calculate a much more effectively constrained best-fitting SED, which is displayed in Fig. 4. The better constraints on the SED morphology then enable more accurate estimates of the stellar mass of the counterpart galaxy.

In Smith & Jarvis (2007), uncertainties in the data meant that the choice of template SEDs used for the SED fitting was not crucial; using either the Maraston (2005) or Bruzual & Charlot (2003) template SEDs made little difference to the outcome. This is no longer the case due to our new IR and millimetre-wavelength data, combined with deeper optical data obtained from the William Herschel Telescope's prime focus imager (PFIP) to investigate the environment of the LAB (Smith & Jarvis, in preparation). The difference between the two models (caused by different treatments of thermally pulsing asymptotic giant branch – TP-AGB – stars) at rest-frame near-IR wavelengths becomes important due to the quality of our IRAC observations. The Maraston models are generally redder, and the effects of the TP-AGP manifest themselves as increased flux at near-IR wavelengths (e.g. Maraston 2005). Since the models vary, we used both sets to approximate our SED. In order to enable reasonable comparisons between the best-fitting models of each type, we required that both fits made use of the Salpeter (1955) initial mass functions (IMFs).

The best-fitting SED was calculated for both species of simple stellar population (SSP) models with ages less than the 3 Gyr (the age of the Universe at $z = 2.83$ in our adopted cosmology is 2.344 Gyr – the reason for this range of SSP ages will become clear), using a simple χ^2 fitting algorithm. We normalized the composite SED to the IRAC 3.6 μm data point (channel 1), since it has the smallest photometric errors of all bands, and is less susceptible to the effects of dust than observations in any of the shorter wavelength bands. A variety of composite stellar SEDs were fit to our LAB counterpart photometry (Table 1), consisting of linear combinations of young (<600 Myr) and old (>600 Myr) simple stellar populations. The best-fitting models based on the Bruzual–Charlot and Maraston SSPs are displayed in Fig. 4.

Whilst the properties of the two fits appear similar, the underlying properties are significantly different. The best-fitting Bruzual & Charlot (2003) composite fit consists of a linear combination of components aged 10 Myr and 0.8 Gyr, with Salpeter IMFs (Salpeter 1955) and solar metallicity. The best-fitting Maraston (2005) model comprises components aged 10 Myr and 2.0 Gyr with Salpeter IMFs, and low metallicity ($Z = 0.0001 = 1/50\,Z_\odot$). The two best-fitting models differ widely in their properties in all but the broadest sense (that the best fit consists of a composite simple stellar population with both young and old components).

Whilst the metallicities appear widely different, the discrepancy in values of χ^2 parameter suggests that our data are not capable of effectively distinguishing between different values of Z. Whilst the best-fitting Maraston (2005) model has $Z = 0.0001$ and $\chi^2 = 10.16$, if we set $Z = 0.02 = Z_\odot$ then the best-fitting model has $\chi^2 = 13.19$ (albeit with a different combination of SSPs – 10 Myr and 3.0 Gyr, older than the age of the Universe at $z = 2.83$). With the data available to us, attempts to effectively constrain values of the host galaxy's metallicity are uncertain.

Table 2. Properties of the best-fitting composite SSPs for both the Bruzual & Charlot (2003) and Maraston (2005) models. The age, masses and errors are presented for both of the SSPs that best fit our extensive photometry.

Parameter	Bruzual & Charlot (2003)	Maraston (2005)
Age_1 (Myr)	10	10
$Mass_1 (M_\odot)$	$9.06 \pm 0.34 \times 10^8$	$5.88 \pm 0.22 \times 10^8$
Age_2 (Gyr)	0.8	2.0
$Mass_2$ ($M_\odot$)	$3.41 \pm 0.13 \times 10^{11}$	$4.35 \pm 0.16 \times 10^{11}$
$Mass_{total}$ ($M_\odot$)	$3.42 \pm 0.13 \times 10^{11}$	$4.36 \pm 0.16 \times 10^{11}$
Best χ^2	7.24	10.16

The masses of each component were derived from the normalizations of the models used in the χ^2 fitting process. The mass of the Bruzual & Charlot (2003) best-fitting model is $3.42 \pm 0.13 \times 10^{11}\,M_\odot$, while for the Maraston (2005) models the total mass is $4.36 \pm 0.16 \times 10^{11}\,M_\odot$. Here, the errors are derived from the normalization based upon the IRAC 3.6 μm flux, and are probably underestimates as a result. The details of each best-fitting population, including masses, ages and errors are shown in Table 2.

Since the old SSP in the Maraston model-fitting scheme is older (2 Gyr) than the old SSP used in the best fit in the Bruzual–Charlot scheme, one would expect it to be more quiescent. That being the case, a larger stellar mass would be required to produce the same luminosity due to the death of the more luminous (and *shorter lived*) stars. The different mass estimates from the Bruzual & Charlot (2003) and Maraston (2005) schemes are not unexpected, since one of the main disagreements between these two models of SEDs relates to the stellar masses implied (e.g. Maraston 2005).

The variation of best-fitting χ^2 as a function of input models is displayed in Fig. 5 for the two fitting regimes. A clear minimum occurs for the combination of 10 Myr and 0.8 Gyr Bruzual & Charlot templates. The preference for this model over other similar combinations is small, but this combination is the best fit, in agreement

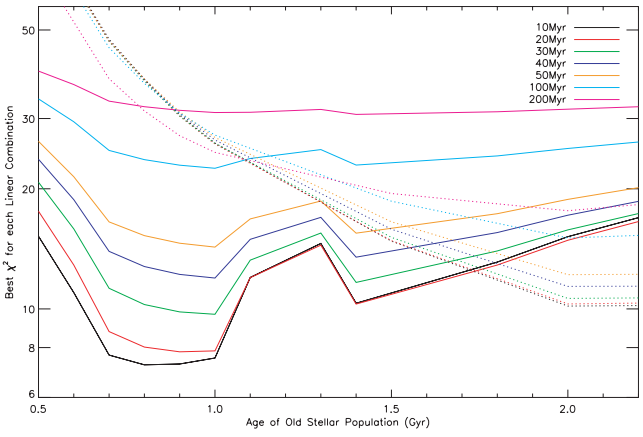

Figure 5. The distribution of best-fitting values of χ^2 for composite Bruzual & Charlot (2003) and Maraston (2005) SSPs (solid and dotted lines, respectively). The age of the best-fitting old SSP component is shown on the abscissa, with the age of the best-fitting young SSP component represented by the colours (see key).

with the results of Smith & Jarvis (2007), which suggested that the counterpart galaxy was best described by a combination of a young and an old simple stellar population. The Bruzual & Charlot models (2003 – solid lines) better approximate our data than those of Maraston (2005 – dotted lines), reflected by the lower values of χ^2. Maraston models older than the age of the Universe are included in this analysis due to the coarse sampling of population ages above 1.5 Gyr, to enable the models to demonstrate a minimum χ^2 value. Thus, we conclude that the host galaxy is well described by a composite simple stellar population, with little or no evidence for additional (e.g. AGN) components. We also note that the composite stellar population is considerably (i.e. orders of magnitude) less luminous between 200 and 912 Å than the Elvis et al. (1994) AGN SED, and therefore also incapable of powering the Lyman α halo.

4 CONCLUSIONS

With our new IRAC, MIPs and MAMBO-2 data, as well as our new deep *U*-, *B*- and *V*-band observations, we have demonstrated that the counterpart galaxy associated with the newly discovered LAB announced in Smith & Jarvis (2007) is well described by a composite stellar population. Using these new multiwavelength data set, we find no plausible evidence for the presence either of an obscured active galactic nucleus or of an energetic starburst that would be required to ionize the neutral hydrogen gas in galaxy-wide superwind schemes. The most likely source of ionization for this particular highly luminous Lyman α halo is a 'cold accretion' scenario, which may be able to supply sufficient energy for this profuse emission without invoking either of the other power sources suggested in the literature (see Fardal et al. 2001; Dijkstra et al. 2006a,b; Dijkstra 2007). We also place further constraints on the host galaxy, and find it to be well described by composite simple stellar populations with total masses of $3.42 \pm 0.13 \times 10^{10}$ or $4.36 \pm 0.16 \times 10^{11}$ $M_{\odot}$, depending on the models used.

ACKNOWLEDGMENTS

DJBS wishes to thank Chris Simpson for valuable conversations, and the UK STFC for a PDRA. MJJ acknowledges the support of a Research Council UK fellowship. This work is based, in part, on observations made with the *Spitzer Space Telescope*, which is operated by the Jet Propulsion Laboratory, California Institute of Technology under a contract with NASA. Support for this work was provided by NASA. Many thanks to the IRAM staff for their support, particularly Stéphane Leon for running the MAMBO pool, and to all guest observers during the pool observing sessions at the 30 m. IRAM is supported by INSU/CNRS (France), MPG (Germany) and IGN (Spain). The Isaac Newton and William Herschel Telescopes are operated on the island of La Palma by the Isaac Newton Group in the Spanish Observatorio del Roque de los Muchachos of the Instituto de Astrofísica de Canarias.

REFERENCES

Antonucci R., 1993, ARA&A, 31, 473
Barrio E. et al., 2008, arXiv:0806.3688
Bruzual G., Charlot S., 2003, MNRAS, 344, 1000
Chapman S. C., Richards E. A., Lewis G. F., Wilson G., Barger A. J., 2001, ApJ, 548, L17
Dey A. et al., 2005, ApJ, 629, 654
Dijkstra M., 2007, preprint (arXiv:0711.2698)
Dijkstra M., Haiman Z., Spaans M., 2006a, ApJ, 649, 14
Dijkstra M., Haiman Z., Spaans M., 2006b, ApJ, 649, 37
Dunkley J. et al., 2008, preprint (arXiv:0803.0586)
Elvis M. et al., 1994, ApJS, 95, 1
Fadda D. et al., 2006, AJ, 131, 2859
Fardal M. A., Katz N., Gardner J. P., Hernquist L., Weinberg D. H., Romeel D., 2001, ApJ, 562, 605
Geach J. E., Smail I., Chapman S. C., Alexander D. M., Blain A. W., Stott J. P., Ivison R. J., 2007, ApJ, 655, L9
Haiman Z., Rees M. J., 2001, ApJ, 553, 545
Haiman Z., Spaans M., Quataert E., 2000, ApJ, 537, L5
Kennicutt R. C., 1998, ARA&A, 36, 189
Kreysa E. et al., 1998, SPIE, 3357, 319
Lacy M. et al., 2004, ApJS, 154, 166
Lacy M. et al., 2005, ApJS, 161, 41
Lacy M., Petric O., Sajina A., Canalizo G., Storrie-Lombardi L. J., Armus L., Fadda D., Marleau F. R., 2007, AJ, 133, 186
Marleau F. et al., 2004, ApJS, 154, 66
Maraston C., 2005, MNRAS, 362, 799
Martínez-Sansigre A., Rawlings S., Lacy M., Fadda D., Marleau F. R., Simpson C., Willott C. J., Jarvis M. J., 2005, Nat, 436, 666
Martínez-Sansigre A. et al., 2007, MNRAS, 379, L6
Matsuda Y. et al., 2004, AJ, 128, 569
Matsuda Y., Iono D., Ohta K., Yamada T., Kawabe R., Hayashino T., Peck A. B., Petitpas G. R., 2007, ApJ, 667, 667
Neugebauer G. et al., 1980, ApJ, 238, 502
Nilsson K. K., Fynbo J. P. U., Møller P., Sommer-Larsen J., Ledoux C., 2006, A&A, 452, 23
Ohyama Y. et al., 2003, ApJ, 591, 9
Oke J. B., Gunn J. E., 1983, ApJ, 266, 713
Omont A., Beelen A., Bertoldi F., Cox P., Carilli C. L., Priddey R. S., McMahon R. G., Isaak K. G., 2003, A&A, 398, 857
Pei Y. C., 1992, ApJ, 395, 130
Polletta M. et al., 2006, ApJ, 642, 673
Salpeter E. E., 1955, ApJ, 121, 161
Seymour N. et al., 2007, ApJS, 171, 353
Siebenmorgen R., Krügel E., 2007, A&A, 461, 445
Siebenmorgen R., Freudling W., Kruegel E., Haas M., 2004, A&A, 421, 129
Smith D. J. B., Jarvis M. J., 2007, MNRAS, 378, L49
Steidel C. C., Adelberger K. L., Shapley A. E., Pettini M., Dickinson M., Giavalisco M., 2000, ApJ, 532, 170
Taniguchi Y., Shioya Y., 2000, ApJ, 532, L13
Villar-Martín M., 2007, New Astron. Rev., 51, 194
Villar-Martín M., Tadhunter C., Morganti R., Holt J., 2005, MNRAS, 359, 5
Weidinger M., Møller P., Fynbo J. P. U., 2004, Nat, 430, 999
Weidinger M., Møller P., Fynbo J. P. U., Thomsen B., 2005, A&A, 436, 825
Wilman R. J., Gerssen J., Bower R. G., Morris S. L., Bacon R., de Zeeuw P. T., Davies R. L., 2005, Nat, 436, 227
Zylka R., 1998, MOPSI Users Manual. IRAM, Grenoble

This paper has been typeset from a TEX/LATEX file prepared by the author.